300 GHz Wireless Link Based on Whole Comb Modulation of Integrated Kerr Soliton Combs

Tomohiro Tetsumoto and Antoine Rolland

***Abstract*—A Kerr microresonator frequency comb, combined with an ultrafast photodiode, has been utilized to generate millimeter- and terahertz-waves with low-phase-noise. This new light source shows promise for wireless communication above the 100 GHz band, where a high signal-to-noise ratio carrier signal is necessary to achieve high data rates. In this study, two efficient wireless link architectures based on a microresonator comb are demonstrated. The experiment shows that simultaneous modulation and detection of multiple comb lines leads to more than 10 times stronger modulation signal strength compared to two-line detection at the receiver. The successful transmission of complex modulation formats up to 64 quadrature amplitude modulation confirms that the microresonator comb and the proposed modulation method are effective for modern wireless communication.**

***Index Terms*—Microresonator, frequency comb, wireless communication.**

I. Introduction

With the continuous exponential growth of data traffic in wireless networks [1], there has been a rise in the development of wireless communication technologies operating above the 100 GHz band, where there are ample frequency resources available [2]. Four frequency bands with a total bandwidth of 137 GHz between 275 GHz and 450 GHz were identified for implementing land mobile and fixed service applications a few years ago [3]. Data rates of 100 Gbit/s have been achieved at the frequency ranges by employing quadrature amplitude modulation (QAM) such as 16-QAM [4], [5], [6], [7]. A simple approach to further progress in data rates while keeping the same bandwidth occupancy is exploiting higher modulation orders. A larger signal-to-noise ratio (SNR) is required in detected signals, which demands higher power and a lower white phase noise floor in carrier signals [8].

Two main methods for generating and modulating/demodulating high-frequency radio frequency (RF) waves with low phase noise exist: all-electronics and photonics-based approaches. The all-electronics approach completes all signal handling processes in electronic circuits. In terms of monolithic integrability, which is a crucial factor for mass production and cost reduction, the all-electronics approach is one step ahead of the photonics-based counterpart. Nonetheless, the multi-stage frequency multiplication and amplification processes that are necessary for generating high-frequency RF waves inherently deteriorate their phase noise and signal-to-noise ratio (SNR), thereby imposing a limitation on the maximum data rate that can be transmitted. The carrier signal is typically modulated with the data stream in the modulation process. In contrast, a photonics-based approach is well-suited for generating lower phase-noise waves. This method utilizes heterodyne detection of optical lines with a fast photodiode (PD) to produce high-frequency RF waves [9]. The phase noise is not restricted by the frequency of the generated wave, but by the relative phase noise of the seed light. This can be controlled independently of the photo-mixing process. Furthermore, sophisticated modulation schemes in optical communication allow for signal encoding in the optical domain. The signal reception is performed using pure electronic or optoelectronic devices [10]. However, systems aiming to achieve ultra-low phase noise tend to be bulky. Additionally, the output power is constrained by the maximum currents that a PD can handle and the PD's responsivity. Two typical examples of photonic oscillators are one based on two stabilized continuous-wave (CW) lasers [11], [12] and one based on an optical frequency comb [9], [13]. The former simply photo-mixes two optical lines where the output frequency is controlled by tuning the laser frequencies. Measuring the absolute output frequency usually requires optical frequency combs [14]. On the other hand, the latter samples two comb lines, whose frequency difference is close to a target frequency, with optical bandpass filters and sends them to a fast PD. The advantages are that determining absolute output frequency and the significant phase noise reduction via the optical frequency division is possible by employing a self-referenced optical frequency comb. For example, the phase noise of about < -120 dBc/Hz at 10 kHz offset has been achieved for a 100 GHz carrier [13]. However, the method suffers from relatively low output SNR due to the low SNR of optical comb lines and the optical loss during comb filtering.

A Kerr microresonator frequency comb [15], [16], also known as a microcomb, is a potential solution to the challenges faced by conventional photonics-based oscillators. This technology generates a repetition frequency between 10 GHz and 1 THz and has demonstrated the ability to produce RF waves with frequencies above 100 GHz via direct detection of comb lines with ultra-fast photodiodes [17], [18], [19], [20], [21]. Using a microcomb in wireless communication offers three main advantages. Firstly,

Manuscript received 9 June 2023; revised 17 September 2023; accepted 10 October 2023. Date of publication 17 October 2023; date of current version 6 November 2023. *(Corresponding author: Tomohiro Tetsumoto.)*

Tomohiro Tetsumoto is with the National Institute of Information and Communications Technology, Koganei 184-8795, Japan.

Antoine Rolland is with IMRA America, Longmont, CO 80503 USA.

Digital Object Identifier 10.1109/JPHOT.2023.3325088

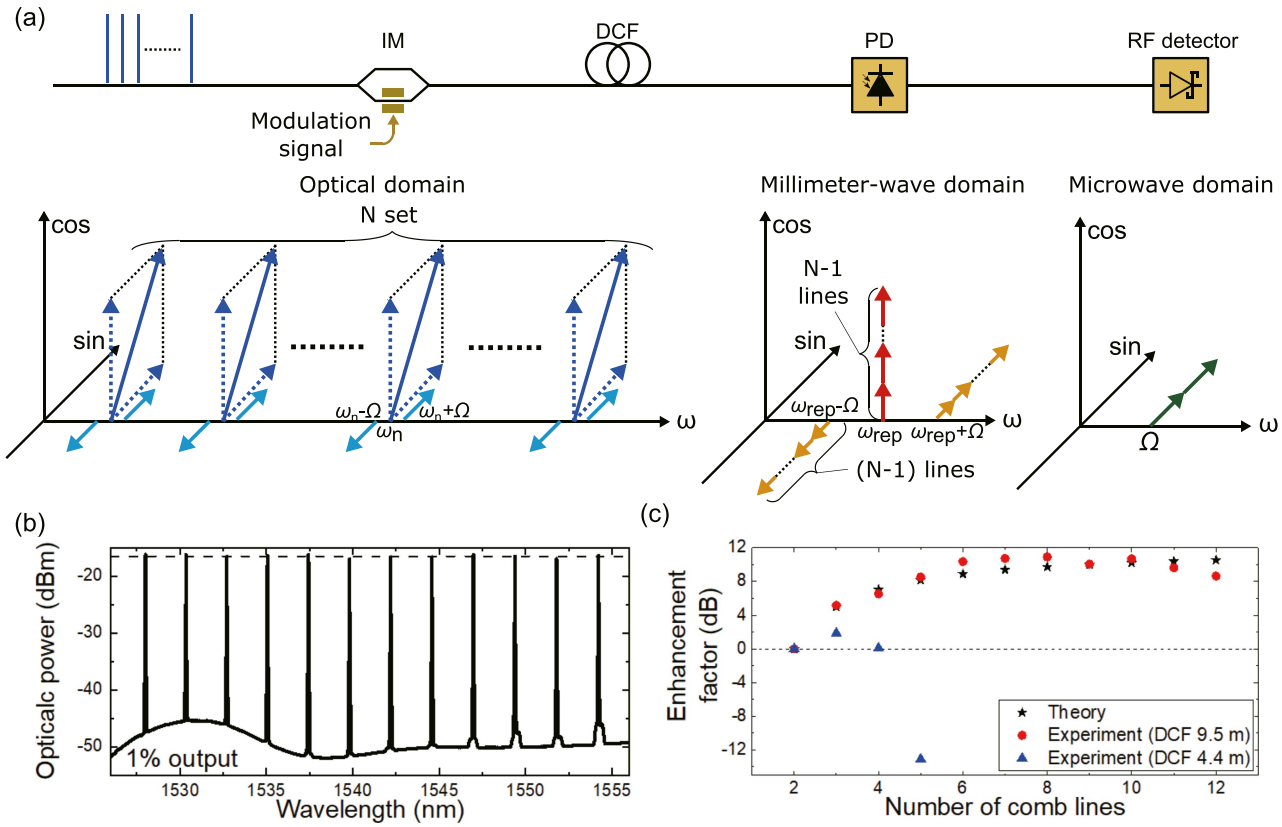

Fig. 1. (a) Schematic illustration of operation principle. The upper half shows an experimental situation considered, and the lower half is the spectrum of signals at each stage. (b) Equalized comb lines from a 1% monitor port after the amplification. The power difference between combs is less than ± 0.5 dB (dashed line). (c) Measured enhancement of detected modulation signal strength. The dashed line shows 0 dB of enhancement.

it is more compact and simpler than other photonics-based oscillators, requiring fewer optical components. Secondly, its phase noise can be significantly reduced through stabilization to microwave references or optical fibers [17], [19], [22], optical frequency division [21], dispersion engineering of microresonators [23], or turning experimental parameters [24], [25]. As a matter of fact, it has enabled the generation of a 300 GHz wave with unprecedented phase noise level [21]. Thirdly, it can enhance the detected modulation signal power through constructive interference of multiple RF waves generated from multiple comb lines. This helps to achieve higher SNR from the limited photocurrent that a photodiode can handle. The main objectives of this study are to describe the principle of the third advantage, to demonstrate its proof-of-concept experimentally, and to show its compatibility with conventional signal handling schemes in wireless communication. The third advantage is demonstrated by modulating power-equalized multiple comb lines, resulting in more than 10 dB enhancement of modulation signal strength compared to a two-line case.

The study confirms successful transmission of up to 64-QAM signal using a microcomb-based 300 GHz transmitter and receiver, whose limitation is not given by the microcomb. The results of this study provide insights into the design of compact transceivers based on microcomb-based photonic millimeter- and terahertz-wave technology, which could be useful for achieving higher data rates in future wireless communication systems.

II. Operation Principle

We modulate the whole comb spectrum and detect it directly in this study. By doing so, the detected modulation signal power is enhanced compared to two-line heterodyne detection under the same photocurrent. Non-modulated cases have been demonstrated in previous studies for carrier signal power enhancement [20], [26].

Power spectrum of photocurrent from a PD of $|I_{\mathrm{PD}}(\omega)|^2$ is given by,

$$|I_{\mathrm{PD}}(\omega)|^2 = |G(\omega) \cdot P(\omega)|^2, \tag{1}$$

where ω is angular frequency, $|G(\omega)|^2$ and $|P(\omega)|^2$ are power spectra of impulse response of a PD and an input wave, respectively. So, the products of the PD output will be proportional to the square of the input wave power spectrum, assuming the PD's response is homogeneous and linear over the frequency of interest. Fig. 1(a) illustrates the modulation/detection methods and spectra obtained at the respective stages. The input is power-equalized N comb lines with amplitude of $1/\sqrt{N}$ normalized so that total power becomes 1. They are modulated with an intensity modulator (IM) with a modulation signal $\phi_{\mathrm{RF}} = M \sin \Omega t$,

where Ω is an RF frequency, and M is modulation depth. There is no in-balance in the optical splitting and combining processes in the IM, and the light only on one arm experiences the modulation. Then, the output of the modulator E_{out} is [27],

$$\begin{aligned} E_{\text{out}} &= \sum_{n=1}^{N} \frac{1}{\sqrt{N}} \left[\cos \omega_n t + \sum_{k=-\infty}^{\infty} J_k(M) \sin\{(\omega_n + k\Omega)t\} \right] \\ &\sim \sum_{n=1}^{N} \frac{1}{\sqrt{N}} [\cos \omega_n t - J_1(M) \sin\{(\omega_n - \Omega)t\} \\ &\quad + J_0(M) \sin \omega_n t + J_1(M) \sin\{(\omega_n + \Omega)t\}] \\ &= \sum_{n=1}^{N} \frac{1}{\sqrt{N}} A_{\text{n}}, \end{aligned} \tag{2}$$

where n and k are integers, ω_n is the angular frequency of n th comb mode, J_k is k th-order Bessel function of the first kind, and A_{n} is the sum of the center and sideband modes around n-th optical line. The factor $1/2$, which explains power splitting and combining, is omitted, and the phase difference between the two arms of $\pi/2$ is assumed for simplicity. Higher order sidebands are neglected since the modulation depth M is small, and $J_{-k} = (-1)^k J_k$ is employed. The left bottom of Fig. 1(a) depicts the optical spectrum of the comb lines at the IM output. These optical lines are sent to a PD and generate a carrier and its sidebands (modulation tones) in the millimeter-wave domain through $I_{\text{PD}} \propto |E_{\text{out}}|^2$. A certain length of a dispersion compensating fiber (DCF) may need to be inserted into the optical path to compensate for the effect of dispersion and align the phase of microcomb lines. The millimeter-wave carrier with the angular repetition frequency $\omega_{\text{rep}} = \omega_n - \omega_{n-1}$ and its sidebands are generated through the interference between adjacent optical lines and their sidebands of,

$$I_{\text{adj}} = \frac{1}{N} \sum_{n=1}^{N-1} A_n A_{n+1}. \tag{3}$$

Each term of (3) gives the following components for the respective angular frequencies when the optical lines are phase-coherent:

$$\begin{aligned} \omega_{\text{rep}} &: \frac{1}{2N}\{1 - J_0^2(M) - 2J_1^2(M)\} \cos \omega_{\text{rep}} t, \\ \omega_{\text{rep}} - \Omega &: -\frac{J_1(M)}{N} \sin\{(\omega_{\text{rep}} - \Omega)\, t\}, \\ \omega_{\text{rep}} + \Omega &: \frac{J_1(M)}{N} \sin\{(\omega_{\text{rep}} + \Omega)\, t\}. \end{aligned}$$

The resulting spectrum around the carrier is schematically shown in the center bottom of Fig. 1(a), where higher-order sidebands are neglected because they are small in the weak modulation condition considered. The amplitude of each frequency component is multiplied by $N - 1$ owing to the contribution from each combination in (3). The envelope of the generated millimeter-wave can be captured with an RF detector, such as a Schottky barrier diode (SBD). The modulation signal $P_{\text{mod}}(N)$ with the angular frequency of Ω is detected in the microwave domain via the interaction between the carrier and the two sidebands, which is expressed as,

$$\begin{aligned} P_{\text{mod}}(N) &\propto 2 \times \frac{N-1}{2N}\{1 - 2J_1(M)^2 - J_0(M)^2\} \\ &\quad \times J_1(M) \frac{N-1}{N} \times \frac{\sin \Omega t}{2} \\ &= \frac{1}{2} \left(\frac{N-1}{N} \right)^2 \\ &\quad \{1 - 2J_1^2(M) - J_0^2(M)\} J_1(M) \sin \Omega t. \end{aligned} \tag{4}$$

Therefore, the enhancement factor of the modulation signal's power spectrum owing to the multiple comb lines can be expressed as follows:

$$|P_{\text{mod}}(N)|^2 \propto \left| \left(\frac{N-1}{N} \right)^2 \right|^2 = \left(\frac{N-1}{N} \right)^4. \tag{5}$$

So, the modulation signal power will be enhanced by $|P_{\text{mod}}(N)|^2/|P_{\text{mod}}(2)|^2 = 16(\frac{N-1}{N})^4$ compared to two-line cases, which will become 16 times (12 dB) when $N \to \infty$. This number is from the 6 dB respective power enhancement of the carrier and sidebands in the millimeter-wave domain. The key point is that each adjacent comb line pair produces an identical set of RF waves regarding amplitudes, frequencies, and phases at the detection. Thus, the principle will be valid for modulation methods that gives the carrier and its sideband signals via photo-detection as long as the optical comb lines are phase-locked and the generated waves interfere constructively.

We demonstrate a simple experiment to confirm the effect. We prepare microcomb lines with a 300 GHz frequency spacing and equalized power by using a waveshaper and an erbium-doped fiber amplifier (EDFA), as shown in Fig. 1(b). They are modulated by a 1.5 GHz sinusoidal wave with an IM and sent to an unitravelling-carrier photodiode (UTC-PD). The envelope of the generated 300 GHz wave is detected with an SBD. A DCF (DCF-38 Thorlabs with $\sim$−38 ps/nm·km) is inserted between the waveshaper and the UTC-PD to compensate for the dispersion effect. We change the number of comb lines to inject, and record the change in the detected signal power of the modulation tone. The photocurrent of the UTC-PD is kept at 0.5 mA for all measurements. Fig. 1(c) shows the results measured with two different DCF lengths, where they are normalized by the power at $N = 2$. With the DCF of 9.5 m (red circle plots), the power of the detected modulation signal increases as the number of comb lines increases, and the trend is close to the theoretical expectation (black star plots). The enhancement factor of as high as 10.9 dB is obtained with 7 comb lines. On the other hand, the signal strength does not go up so high with increased numbers of comb lines but drops significantly with a 4.4 m DCF (blue triangular plots, at $N = 5$), where the dispersion of the optical path is not compensated correctly (the group delay time is estimated to be about 0.36 ps/nm in the optical path since the 9.5 m DCF approximately compensates for it). This presents that appropriate comb line phase alignment is important for the multiple comb line detection scheme [20]. The effect of the dispersion also can be seen in the plots for 9.5 m DCF at $N > 9$.

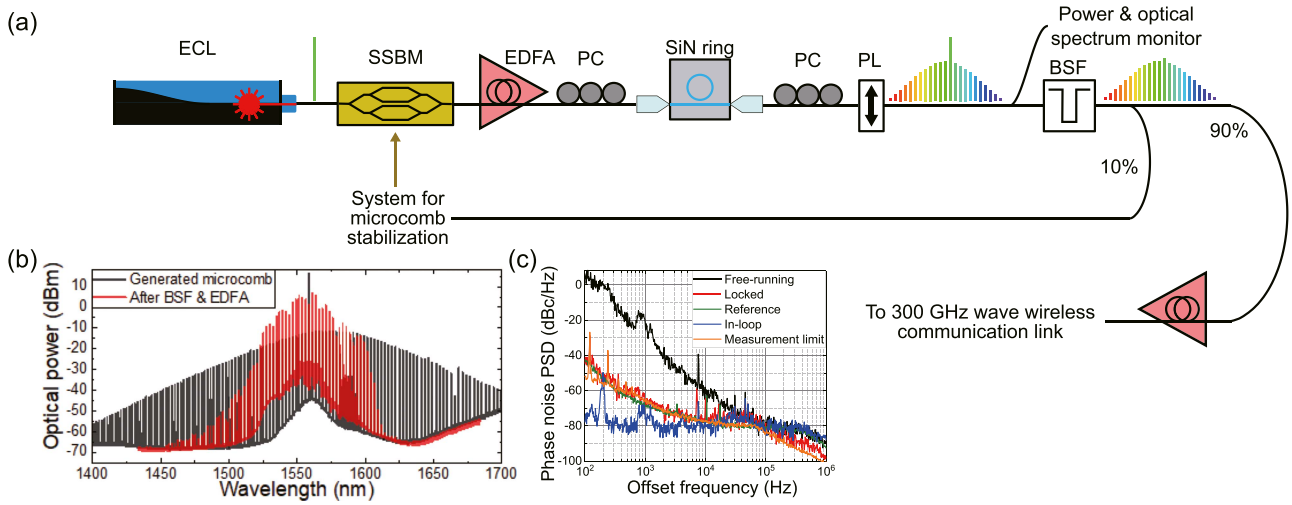

Fig. 2. (a) Schematic drawing of the experimental setup for microcomb generation and stabilization. See text for details. (b) Generated microcomb's optical spectra. (c) Microcomb phase noise.

III. Microcomb Generation, Stabilization & Characterization

IV. Wireless Communication Experiments

Fig. 2 depicts an experimental setup for microcomb generation and stabilization. Single sideband modulation is applied to CW light from an external cavity laser diode (ECL, Toptica CTL1550) with a single sideband modulator (SSBM), and the output is amplified with an EDFA. The light is coupled with a ring resonator made of silicon nitride (SiN) after polarization alignment using a polarization controller (PC). The loaded quality factor of the resonator is about 2×10^6. A soliton microcomb is excited by fast scanning the strong pump light with the SSBM [28], [29]. The generated microcomb is polarized with another PC and a polarizer (PL). We employ polarization-maintaining fibers after here. A small portion of the comb light is sampled for power and spectrum monitoring during the experiment. The pump light is suppressed with a bandstop filter (BSF), and the output is split into two paths with a 90:10 optical coupler. The 90% of the light is amplified with an EDFA and sent to a wireless link, explained later. Fig. 2(b) shows the optical spectra of the generated microcomb and the filtered and amplified comb on the 90% port. The bandwidth of the filtered comb spectrum is mainly limited by the BSF and EDFA gain bandwidths. Pump-to-comb conversion efficiency is estimated to be ~4% from the ratio between the pump power and the total power of the other combs in the optical spectrum. The output from the 10% port is used to stabilize the microcomb through the method described in [19]. By applying a control signal to the SSBM, the microcomb is stabilized to a clock signal at microwave frequency domain to suppress the frequency drift. Fig. 2(c) shows the phase noise of the microcomb. The free-running noise (black) is suppressed down to the reference noise (green) when the phase-locking is activated (red). The stabilized microcomb noise is limited by the in-loop noise (blue) between around 20 kHz and 100 kHz offset.

Wireless communication systems in this study consist of software and hardware parts; the former is for producing and analyzing digital signals, and the latter is for modulating, transmitting, and receiving 300 GHz waves. Digital signal processing (DSP) in the wireless system is performed with MATLAB & Simulink, and transmitter and receiver based on field programmable gate arrays (FPGAs) (USRP N210, Ettu) acting as interfaces between the software and the hardware parts. Fig. 3(a) depicts the schematic of the system. The host computer, which processes the Simulink program, the FPGA transmitter, and the receiver, are connected via Ethernet cables and hubs. The transmitter and the receiver share the same clock signal as the microcomb. The software program generates modulation signals encoded with either 4-QAM, 16-QAM, 64-QAM, or 256-QAM. The center frequency and the symbol rate of the signal are set to 1.5 GHz and 200 kHz, respectively, where the rather low symbol rate is to avoid overrun and underrun in the software-hardware communication. Note that our focus in this study is the proof-of-concept of the transceiver based on all-comb modulation and we do not pursue high-data-rate transmission due to the lack of equipment for that. The transmitter is configured to generate the produced modulation signal as an arbitrary waveform generator. The modulated signal is applied to an intensity modulator (IM) in the hardware system. The in-phase and quadrature-phase components of the signal are superimposed in the RF wave domain. The detected signal in the hardware is down-converted to baseband frequency, digitized in the FPGA receiver, and analyzed with the Simulink program in the host computer in real-time. We evaluated the received signal's root mean square (RMS) error vector magnitude (EVM).

Fig. 3(b)–(e) shows the results of a back-to-back preliminary experiment, where the FPGA transmitter and the FPGA receiver are connected with a 1.5 m electric cable and a 10 dB attenuator. Constellation points can be recognized clearly in 4-QAM, 16-QAM, and 64-QAM cases with EVM of 9.3%, 5.8%, and 7.2%, respectively, whereas 256-QAM constellation with EVM

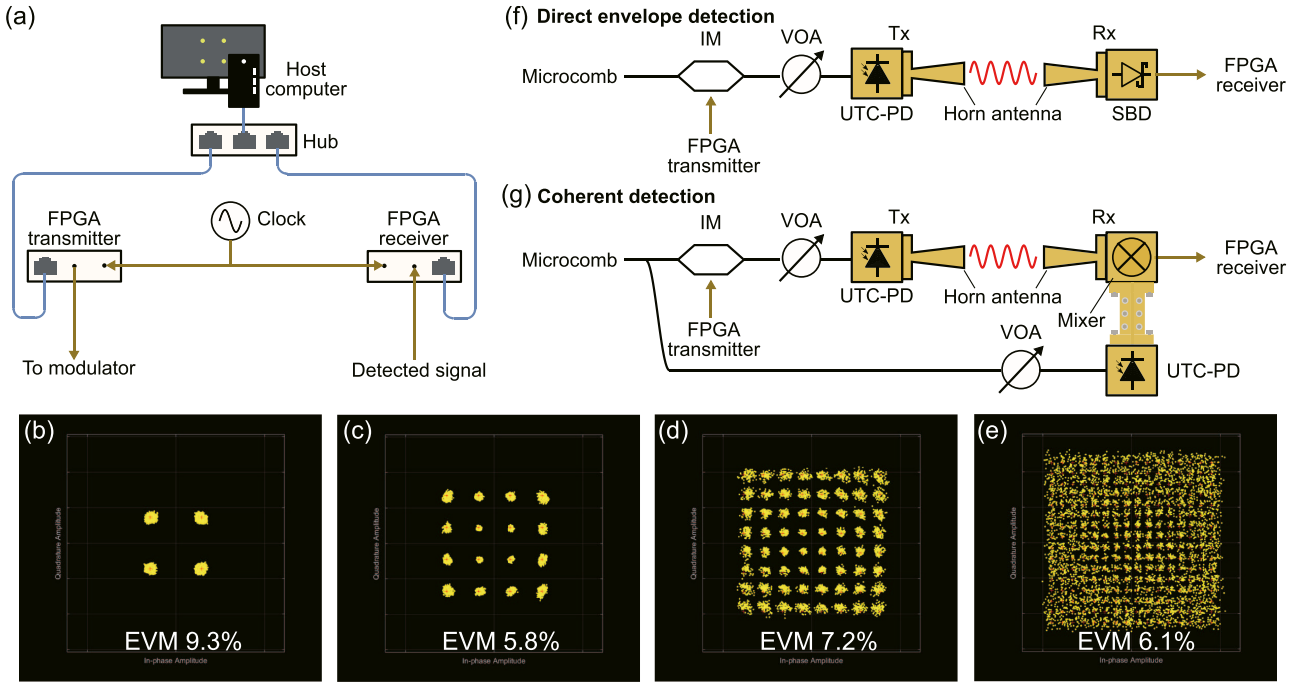

Fig. 3. (a) Schematic drawing of FPGA-based modulation/demodulation system. (b)–(e) Constellation diagrams for 4-QAM, 16-QAM, 64-QAM and 256-QAM modulation schemes, respectively, in FPGA direct link. Schematic drawing of wireless links based on (f) direct envelope detection and (g) coherent detection. See text for details.

of 6.1% is not resolved well. These results pose the lowest levels of the reachable EVM in the following experiments.

We tested two types of wireless links to examine if the proposed microcomb-based modulation scheme is compatible with the standard signal detection methods. One is based on direct envelope detection of the 300 GHz carrier with an SBD (Fig. 3(f)). The stabilized microcomb is modulated by the IM and detected with a UTC-PD, where a 300 GHz carrier is generated. The phase noise of the 300 GHz carrier is the pure copy of the microcomb's repetition rate noise as it is generated via the photo-mixing of the comb lines when there is no significant unpleasant effect at the PD, such as the AM-to-PM conversion. The 300 GHz wave is radiated into free space with a horn antenna, travels 0.1 m, is captured with another horn antenna, and is detected with the SBD. The output from the detector is sent to the FPGA receiver. The other system employs coherent mixing of two 300 GHz waves (Fig. 3(g)). The modulated wave is generated the same way as the direct envelope detection. Another wave for the down-conversion is produced by detecting the same microcomb before the modulation in this proof-of-concept study.

The generated two waves are mixed with a 300 GHz fundamental mixer, and the intermediate frequency (IF) signal is supplied to the FPGA receiver. Although a homodyne detection system requires precise control of the relative phase of two waves detected in general, its fluctuation was slow enough in our experiment owing to the short path length after the fork, and no active control was implemented. Note that we did not use a DCF in the two setups since we can obtain sufficient SNR for the demonstration without it.

Fig. 4(a) presents a picture of the actual wireless link based on direct envelope detection. We employ horn antennas with a designed gain of 26 dBi. The transmittance is maximized by controlling the positions of the antennas with 3-axis mechanical stages. To check the transmission loss, we detect the 1.5 GHz sinusoidal wave modulation signal delivered by a 300 GHz carrier in the 0.1 m link and a 1 mm link. Fig. 4(b) shows the RF spectra of the detected signals. We observe about 13 dB reduction of the SNR through the 0.1 m free-space trip compared to the 1 mm link. Fig. 4(c)–(f) displays the results of the wireless communication. The obtained EVM are 8.6%, 6.3%, 7.1%, and 6.4% for 4-QAM, 16-QAM, 64-QAM, and 256-QAM, respectively. So, no apparent degradation of signal quality is observed compared to the direct FPGA link experiment (Fig. 3(b)–(e)). The wireless link for the coherent detection is presented in Fig. 5(a). Most components are the same as ones in the direct envelope detection system, but the SBD is replaced with a fundamental mixer, and another UTC-PD is attached to it to supply a 300 GHz wave to the LO port. Again, we demonstrate the transmission test and observe a 12 dB decrease in the SNR in the 0.1 m link. The acquired constellation diagrams are shown in Fig 5(c)–(f). EVM of 8.8%, 6.2%, 6.5%, and 6.3% are obtained for 4QAM, 16QAM, 64QAM, and 256QAM, respectively, which are merely limited by the FPGA transmitter and receiver.

Fig. 6 summarises the results of the communication experiments. EVM threshold to obtain bit error ratio (BER) of 4×10^{-3} is displayed by the black dashed line with star symbols as a measure of successful transmission [6], [30]. With the EVM level, the BER will be decreased to 10^{-15} level by the forward error correction with 7% overhead [31]. The obtained EVM

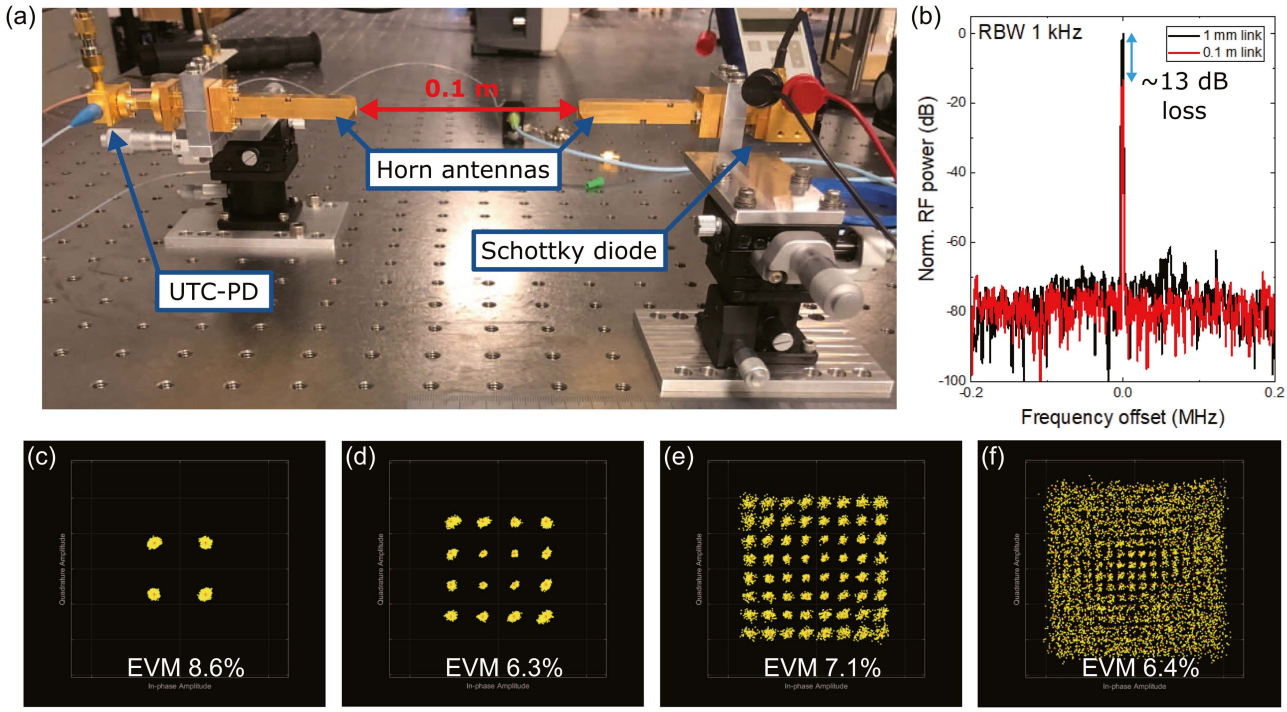

Fig. 4. (a) Picture of the wireless link based on direct envelope detection. (b) RF spectra of detected 1.5 GHz modulated tones in transmission loss test. RBW is 1 kHz. (c)–(f) Constellation diagrams for 4-QAM, 16-QAM, 64-QAM and 256-QAM modulation schemes, respectively, in direct envelope detection.

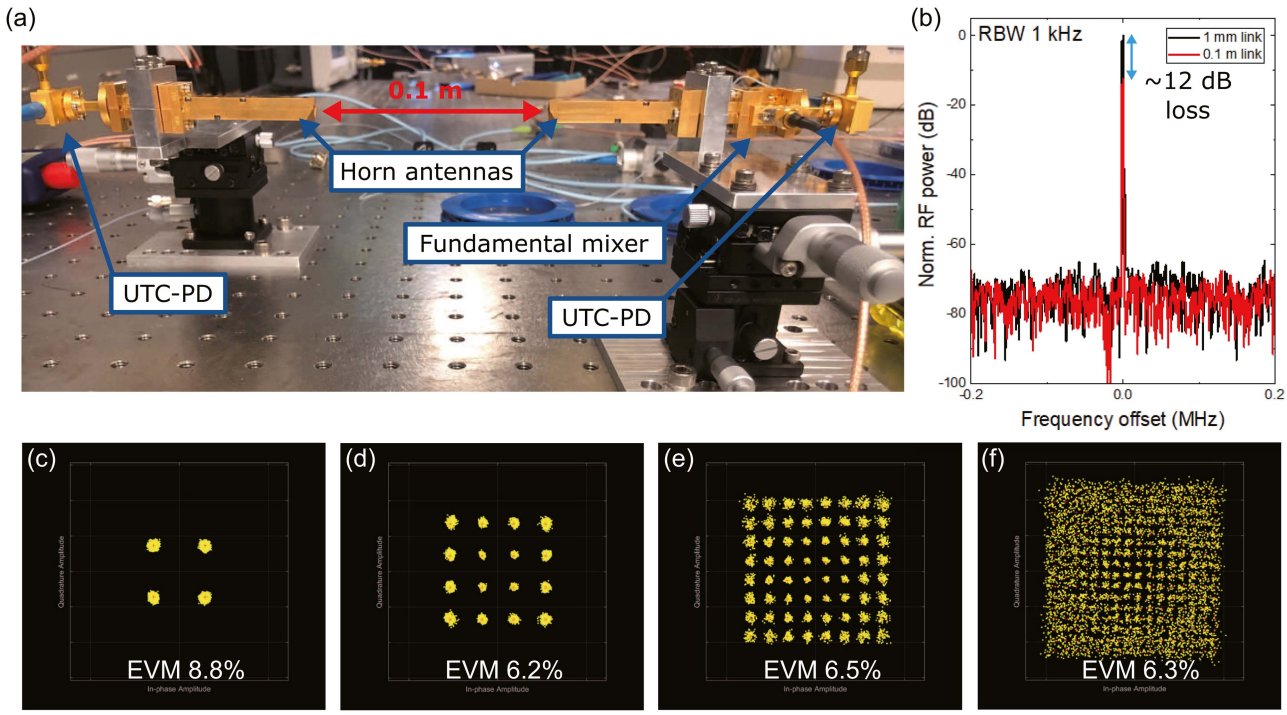

Fig. 5. (a) Picture of the wireless link based on coherent detection. (b) RF spectra of detected 1.5 GHz modulated tones in transmission loss test. RBW is 1 kHz. (c)–(f) Constellation diagrams for 4-QAM, 16-QAM, 64-QAM, and 256-QAM modulation schemes, respectively, in coherent detection.

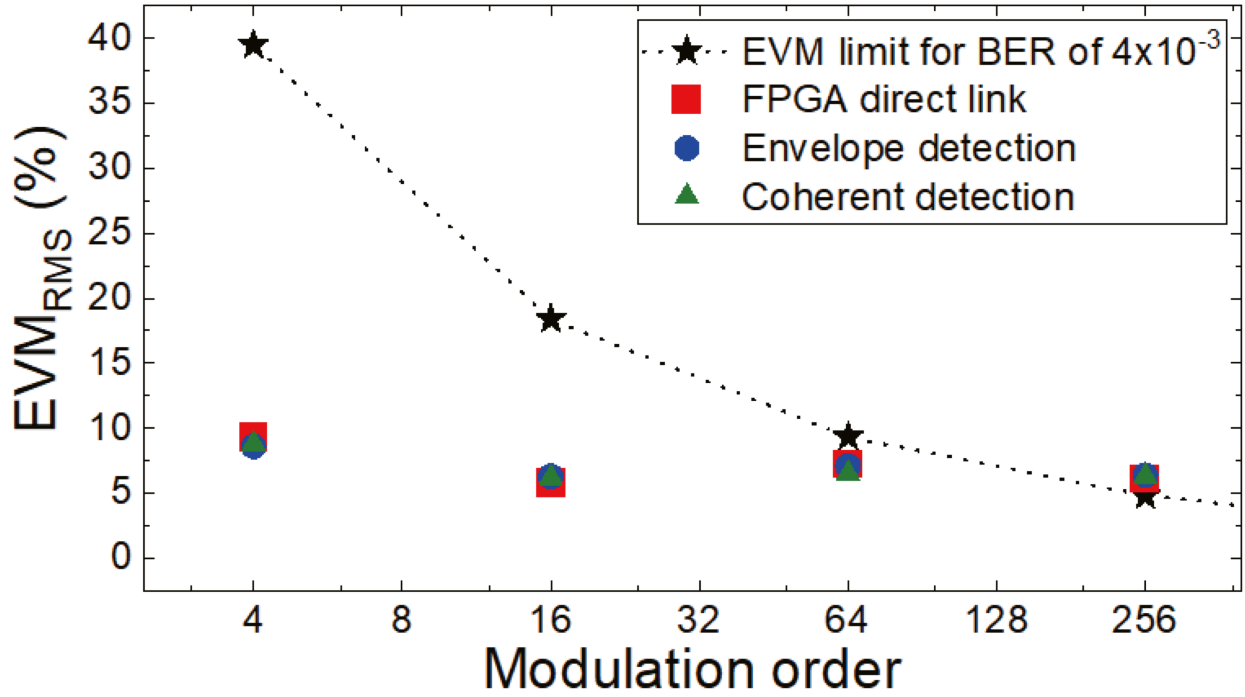

Fig. 6. Summary of obtained EVM in wireless communication experiments.

levels are below the EVM limit in the experiment up to 64-QAM but slightly beyond the limit in the 256-QAM demonstration. The limitation is given by the FPGA transmitter and receiver (phase noise is −80 dBc/Hz at 10 kHz offset for a 1.8 GHz signal according to their specification sheet). This is convincing because the microcomb's phase noise is canceled out and we will see only modulation signal noise at the reception in the two wireless links demonstrated in this study. However, the carrier and LO noise will degrade detected modulation signals in coherent detection practically, where two different oscillators are employed at the transmitter and receiver sides.

V. Discussion & Outlook

Here, we discuss microcomb's advantages for wireless communication and future perspective.

Our experiments demonstrate that a microcomb can be an oscillator in wireless links utilizing complex modulation formats. The system is relatively simple compared to other photonics-based approaches because it starts from a single CW light, and no spectral filtering process is required, which allows comb lines to propagate in a shared path all the time. This is, in particular, a significant difference from photonics-based systems using conventional comb sources, which suffer from large loss due to splitting, filtering, and combining processes and sometimes even require mechanisms to compensate for fluctuation of path length difference [9]. On the other hand, a possible drawback is signal strength attenuation due to the destructive interference between multiple modulation tones generated from different optical line pairs. Such destructive interference may occur even when a comb is mode-locked if modulation sidebands have different phases for different optical lines (i.e., wavelength dependence of sideband phase), where we suppose a standard optical modulator does not give a significant dependence. We have shown that the effect is negligible at a modulation frequency of 1.5 GHz when the comb line's phases are aligned. On the other hand, it has not been confirmed experimentally if it works in the same way when a high data rate is exploited by employing a large modulation bandwidth. Higher data rate transmission experiments will be explored in future works.

Also, the employed two architectures will benefit from respective merits as follows. The direct envelope detection scheme does not require low-phase-noise carriers because the carrier noise will be canceled out at the detection, whereas its sensitivity is limited by a detector employed. So, the critical parameters for this configuration are the noise property of RF sources in modulation/demodulation (e.g., arbitrary waveform generator for encoding, an oscillator for decoding), signal strength at a transmitter, and detector sensitivity. A microcomb will improve the signal strength via the simultaneous modulation and detection of comb lines.

The coherent detection scheme will enhance detection sensitivity by a strong LO signal and give a larger bandwidth at the IF output in general. However, detected SNR will be affected by the phase noise of both RF and LO signals injected into a mixer. Also, the RF and LO signals need to have a small frequency drift or, ideally, share the common clock signals to help carrier frequency and phase synchronization in the DSP work properly. Regarding the former concern about phase noise, a 300 GHz microcomb can be comparable (−100 dBc/Hz at 10 kHz) to an

arbitrary waveform generator at 10 GHz used in a cutting-edge communication experiment [7] (−95 dBc/Hz at 10 kHz offset, Keysight M8196A [32]) through the optical frequency division technique [21]. So far, white phase noise floors of microcombs at 300 GHz are observed at around −120 dBc/Hz limited by shot noise and noise figure of electronic devices [17], [21]. This is still >10 dB lower than that of a typical electronic 300 GHz oscillator based on frequency multiplication [33]. As to the latter concern about clocking, a microcomb oscillator can be stabilized to a clock signal at microwave domain [19], as demonstrated in this study.

Several challenges need to be addressed to realize low-cost and portable microcomb-based transceivers for future wireless communication. For instance, system integration is a critical one. Although a system based on the optical fiber connection like the one in this study can be packaged compactly, making it on-chip is more desirable for miniaturization and mass production. Such a platform will also mitigate dispersion effects, observed in Fig. 1(e), thanks to much shorter path lengths. Hybrid and heterogeneous integration [34], [35] will be a key technology to achieve the goal [36]. Another issue is the required power reduction to obtain strong optical comb lines. The excitation power requirement for the microcomb generation has been lowered through progress in fabrication technologies and theoretical and experimental understanding of its generation physics. For example, a soliton microcomb has been excited with 100-mW-level electrical power (1-mW-level optical power) by employing an ultrahigh Q SiN ring resonator ($Q \sim 10^7$) [37]. Pump-to-comb conversion efficiency is also an important measure to evaluate energy cost. It can be controlled via various parameters such as the resonator's size and loss and coupling between a waveguide and a resonator, where the efficiency close to 10% is predicted for a 300 GHz SiN resonator with intrinsic Q in the order of 10^6 under a highly over-coupled condition [38]. To achieve the efficiency of >10%, using dark pulses or coupled resonator configurations can be effective approaches [39], [40], [41], [42]. Injection locking of two lasers to a microcomb is also an effective approach to amplify the signal strength [43], which is employed in demonstrating wireless communication at 300 GHz with high data rate of 80 Gbps [44].

In this study, we successfully demonstrated the utilization of a microcomb to establish wireless communication links operating at a frequency of 300 GHz. By employing simultaneous modulation of multiple microcomb lines, we were able to significantly enhance the strength of the detected modulation signal by more than 10 dB compared to the scenario where only two lines were modulated. Furthermore, we conducted transmission experiments involving complex modulation formats in two different types of wireless links, utilizing a microcomb that was stabilized to a reference clock. Notably, no degradation in signal quality was observed during these experiments. Moreover, we achieved successful transmission of a high-order QAM signal, specifically a 64-QAM signal, in both wireless links. Overall, our findings suggest that the microcomb holds great promise as a photonic oscillator for augmenting data capacity in future wireless communication systems.

Disclaimer

We notice that a article about wireless communication using microcombs at 560 GHz [45] is published during the manuscript preparation after our preprint publication [46]. We note that there are differences in the research focus between [45] and this study besides the operation frequency and employed modulation format differences. The major contrast is that we explore and elaborate on the principle and benefits of the whole comb modulation scheme, while the signal encoding is based on one comb line modulation in [45].

References

[1] "5G Wireless: Capabilities and challenges for an evolving network," [Online]. Available: https://www.gao.gov/assets/gao-21-26sp.pdf

[2] T. Nagatsuma, G. Ducournau, and C. C. Renaud, "Advances in terahertz communications accelerated by photonics," *Nature Photon.*, vol. 10, no. 6, pp. 371–379, 2016.

[3] "World radiocommunication conference 2019 (WRC-19) final acts," [Online]. Available: https://www.itu.int/dms_pub/itu-r/opb/act/R-ACT-WRC.14-2019-PDF-E.pdf

[4] S. Koenig et al., "Wireless sub-THz communication system with high data rate," *Nature Photon.*, vol. 7, no. 12, pp. 977–981, 2013.

[5] T. Nagatsuma et al., "Real-time 100-Gbit/s QPSK transmission using photonics-based 300-GHz-band wireless link," in *Proc. IEEE Int. Topical Meeting Microw. Photon.*, 2016, pp. 27–30.

[6] V. Chinni et al., "Single-channel 100 Gbit/s transmission using III–V UTC-PDs for future IEEE 802.15. 3D wireless links in the 300GHz band," *Electron. Lett.*, vol. 54, no. 10, pp. 638–640, 2018.

[7] H. Hamada et al., "300-GHz 100-Gb/s InP-HEMT wireless transceiver using a 300-GHz fundamental mixer," in *Proc. IEEE/MTT-S Int. Microw. Symp.*, 2018, pp. 1480–1483.

[8] J. Chen et al., "Influence of white LO noise on wideband communication," *IEEE Trans. Microw. Theory Techn.*, vol. 66, no. 7, pp. 3349–3359, Jul. 2018.

[9] T. Nagatsuma et al., "Terahertz wireless communications based on photonics technologies," *Opt. Exp.*, vol. 21, no. 20, pp. 23736–23747, 2013.

[10] T. Harter et al., "Wireless THz link with optoelectronic transmitter and receiver," *Optica*, vol. 6, no. 8, pp. 1063–1070, 2019.

[11] Y. Li, A. Rolland, K. Iwamoto, N. Kuse, M. Fermann, and T. Nagatsuma, "Low-noise millimeter-wave synthesis from a dual-wavelength fiber brillouin cavity," *Opt. Lett.*, vol. 44, no. 2, pp. 359–362, 2019.

[12] R. Amin, J. Greenberg, B. Heffernan, T. Nagatsuma, and A. Rolland, "Exceeding octave tunable terahertz waves with zepto-second level timing noise," 2022, *arXiv:2207.07750*.

[13] T. Fortier et al., "Optically referenced broadband electronic synthesizer with 15 digits of resolution," *Laser Photon. Rev.*, vol. 10, no. 5, pp. 780–790, 2016.

[14] T. Yasui et al., "Widely and continuously tunable terahertz synthesizer traceable to a microwave frequency standard," *Opt. Exp.*, vol. 19, no. 5, pp. 4428–4437, Feb. 2011. [Online]. Available: https://opg.optica.org/oe/abstract.cfm?URI=oe-19-5-4428

[15] T. Herr et al., "Temporal solitons in optical microresonators," *Nature Photon.*, vol. 8, no. 2, pp. 145–152, 2014.

[16] V. Brasch et al., "Photonic chip–based optical frequency comb using soliton Cherenkov radiation," *Science*, vol. 351, no. 6271, pp. 357–360, 2016.

[17] S. Zhang, J. M. Silver, X. Shang, L. Del Bino, N. M. Ridler, and P. Del'Haye, "Terahertz wave generation using a soliton microcomb," *Opt. Exp.*, vol. 27, no. 24, pp. 35257–35266, 2019.

[18] S.-W. Huang et al., "Globally stable microresonator turing pattern formation for coherent high-power THz radiation on-chip," *Phys. Rev. X*, vol. 7, no. 4, 2017, Art. no. 041002.

[19] T. Tetsumoto, F. Ayano, M. Yeo, J. Webber, T. Nagatsuma, and A. Rolland, "300 GHz wave generation based on a Kerr microresonator frequency comb stabilized to a low noise microwave reference," *Opt. Lett.*, vol. 45, no. 16, pp. 4377–4380, 2020.

[20] B. Wang et al., "Towards high-power, high-coherence, integrated photonic mmwave platform with microcavity solitons," *Light: Sci. Appl.*, vol. 10, no. 1, pp. 1–10, 2021.

[21] T. Tetsumoto, T. Nagatsuma, M. E. Fermann, G. Navickaite, M. Geiselmann, and A. Rolland, "Optically referenced 300 GHz millimetre-Wave oscillator," *Nature Photon.*, vol. 15, pp. 516–522, 2021.

[22] N. Kuse, K. Nishimoto, Y. Tokizane, S. Okada, K. Minoshima, and T. Yasui, "Low noise 560 GHz generation from a fiber-referenced Kerr microresonator soliton comb," in *CLEO: Applications and Technology*. Optica Publishing Group, 2022, Art. no. JW3B–1.

[23] J. R. Stone and S. B. Papp, "Harnessing dispersion in soliton microcombs to mitigate thermal noise," *Phys. Rev. Lett.*, vol. 125, no. 15, 2020, Art. no. 153901.

[24] X. Yi, Q.-F. Yang, X. Zhang, K. Y. Yang, X. Li, and K. Vahala, "Single-mode dispersive waves and soliton microcomb dynamics," *Nature Commun.*, vol. 8, no. 1, pp. 1–9, 2017.

[25] T. Tetsumoto, J. Jiang, M. E. Fermann, G. Navickaite, M. Geiselmann, and A. Rolland, "Effects of a quiet point on a Kerr microresonator frequency comb," *OSA Continuum*, vol. 4, no. 4, pp. 1348–1357, 2021.

[26] F.-M. Kuo et al., "Spectral power enhancement in a 100 GHz photonic millimeter-Wave generator enabled by spectral line-by-line pulse shaping," *IEEE Photon. J.*, vol. 2, no. 5, pp. 719–727, Oct. 2010.

[27] V. J. Urick, K. J. Williams, and J. D. McKinney, *Fundamentals of Microwave Photonics*. Hoboken, NJ, USA, Wiley, 2015.

[28] T. C. Briles et al., "Interlocking Kerr-microresonator frequency combs for microwave to optical synthesis," *Opt. Lett.*, vol. 43, no. 12, pp. 2933–2936, 2018.

[29] N. Kuse, T. C. Briles, S. B. Papp, and M. E. Fermann, "Control of Kerr-microresonator optical frequency comb by a dual-parallel Mach-Zehnder interferometer," *Opt. Exp.*, vol. 27, no. 4, pp. 3873–3883, 2019.

[30] R. A. Shafik, M. S. Rahman, and A. R. Islam, "On the extended relationships among EVM, BER and SNR as performance metrics," in *Proc. IEEE Int. Conf. Elect. Comput. Eng.*, 2006, pp. 408–411.

[31] F. Chang, K. Onohara, and T. Mizuochi, "Forward error correction for 100G transport networks," *IEEE Commun. Mag.*, vol. 48, no. 3, pp. S48–S55, Mar. 2010.

[32] "Keysight technologies M8196A," [Online]. Available: https://www.keysight.com/us/en/assets/7018-04911/data-sheets/5992-0971.pdf

[33] I. Dan, G. Ducournau, S. Hisatake, P. Szriftgiser, R.-P. Braun, and I. Kallfass, "A superheterodyne 300 GHz wireless link for ultra-fast terahertz communication systems," *Int. J. Microw. Wireless Technol.*, vol. 12, no. 7, pp. 578–587, 2020.

[34] D. Liang and J. E. Bowers, "Recent progress in heterogeneous III-V-on-Silicon photonic integration," *Light: Adv. Manuf.*, vol. 2, no. 1, pp. 1–25, 2021.

[35] P. Kaur, A. Boes, G. Ren, T. G. Nguyen, G. Roelkens, and A. Mitchell, "Hybrid and heterogeneous photonic integration," *APL Photon.*, vol. 6, no. 6, 2021, Art. no. 061102.

[36] C. Xiang et al., "Laser soliton microcombs heterogeneously integrated on silicon," *Science*, vol. 373, no. 6550, pp. 99–103, 2021.

[37] B. Stern, X. Ji, Y. Okawachi, A. L. Gaeta, and M. Lipson, "Battery-operated integrated frequency comb generator," *Nature*, vol. 562, no. 7727, pp. 401–405, 2018.

[38] J. K. Jang et al., "Conversion efficiency of soliton Kerr combs," *Opt. Lett.*, vol. 46, no. 15, pp. 3657–3660, 2021.

[39] X. Xue, P.-H. Wang, Y. Xuan, M. Qi, and A. M. Weiner, "Microresonator Kerr frequency combs with high conversion efficiency," *Laser Photon. Rev.*, vol. 11, no. 1, 2017, Art. no. 1600276.

[40] B. Y. Kim et al., "Turn-key, high-efficiency Kerr comb source," *Opt. Lett.*, vol. 44, no. 18, pp. 4475–4478, 2019.

[41] X. Xue, X. Zheng, and B. Zhou, "Super-efficient temporal solitons in mutually coupled optical cavities," *Nature Photon.*, vol. 13, no. 9, pp. 616–622, 2019.

[42] Ó. B. Helgason et al., "Power-efficient soliton microcombs in anomalous-dispersion photonic molecules," in *CLEO: QELS_Fundamental Science*. Optica Publishing Group, 2022, Art. no. FW4J–5.

[43] N. Kuse and K. Minoshima, "Amplification and phase noise transfer of a Kerr microresonator soliton comb for low phase noise THz generation with a high signal-to-noise ratio," *Opt. Exp.*, vol. 30, no. 1, pp. 318–325, 2022.

[44] B. M. Heffernan et al., "60 Gbps real-time wireless communications at 300 GHz carrier using a Kerr microcomb-based source," *APL Photon.*, vol. 8, no. 6, 2023.

[45] Y. Tokizane et al., "Terahertz wireless communication in a 560-GHz band using a Kerr micro-resonator soliton comb," *Opt. Continuum*, vol. 2, no. 5, pp. 1267–1275, 2023.

[46] T. Tetsumoto and A. Rolland, "300 GHz wireless link based on an integrated Kerr soliton comb," 2022, *arXiv:2210.15881*.